

## TWO-DIMENSIONAL KALMAN SMOOTHING FOR DIGITAL TERRAIN MODELLING

Ping Wang\*, John C. Trinder, Shaowei Han\*\*

\*School of Geography, The University of New South Wales, Sydney 2052, Australia,  
[p2179512@saturn.geog.unsw.edu.au](mailto:p2179512@saturn.geog.unsw.edu.au)

\*\*School of Geomatic Engineering, The University of New South Wales, Sydney 2052, Australia,  
[j.trinder@unsw.edu.au](mailto:j.trinder@unsw.edu.au), [s.han@unsw.edu.au](mailto:s.han@unsw.edu.au)

**KEY WORDS:** DTM/DEM/DSM, GIS, Terrain Modelling, Topology

### ABSTRACT

The morphology of the surface of the earth plays an important role in understanding the physical, chemical, and biological processes that occur within the landscape. Terrain elevation, slope, aspect, profile and plan curvature, flow path length, and catchment areas are the 'primary terrain attributes' in geomorphology, which reflect terrain significance and can be directly calculated from a DEM. However, errors in DEMs have a significant impact on the derivation of reliable and accurate terrain attributes. In this paper, a 2-D Kalman smoothing algorithm for digital terrain modelling is introduced to reduce the effect of the DEM random noise and detect and remove the effect of DEM outliers in terrain modelling. The developed 2-D Kalman smoother is a linear combination of the results of 2-D Kalman filtering applied four times for different orientations over the same DEM. The experiments over a simulated DEM show significant improvements in the derivation of the relevant slope surface and aspect surface calculation by the 2-D Kalman smoothing compared with other methods.

### 1 INTRODUCTION

Developments in the automation of terrain analysis and the use of Digital Elevation Models (DEMs) have made possible the quantification of topographic attributes of a landscape. Terrain elevation, slope, aspect, profile and plan curvature, flow path length, and catchment areas are the 'primary terrain attributes' in geomorphology, which can be directly calculated from a DEM, and reflect terrain hydrologic, biological and geographical significance (Moore et al, 1991). They are also the bases, combined with other geographical information, to derive the 'secondary terrain attributes', such as soil water content, precipitation, and solar radiation, which further characterize the spatial variability of specific processes occurring in the landscape.

However, DEMs comprise both random errors and outliers. Random errors are randomly distributing within the DEM, having high frequency characteristics in the spectral domain, and normally zero mean and a certain variance (Tempfli, 1980). DEM outliers are the observations which deviate sufficiently from other observations as to arouse suspicions that they were generated by a different mechanism (Hawkins, 1980). The study of the impact of DEM random errors on the extraction of terrain features reveals that their magnitudes and spatial patterns significantly affect the results of the terrain analysis (Tempfli, 1980, Torlegård et al, 1986, Lee et al, 1992, Kraus, 1994, Li, 1994, Rieger, 1996, Hunter and Goodchild, 1997, Wang, 1998, Wang et al, 1998a, Florinsky 1998). Wang et al (1998b) have pointed out that the effect of DEM outliers on terrain surface modelling is also significant, but few studies had been documented on the quantitative evaluation of their impact.

Reviews of developments in digital terrain modelling (Skidmore, 1989, Chang and Tsai, 1991, Srinivasan and Engel, 1991, Florinsky, 1998, Wang et al, 1999) indicate that nearly all of them are deterministic and are based on a 3 by 3 modelling window, using only a limited number of neighbouring DEM points (up to 9 DEM points) to solve the terrain attributes of the point of interest. This limited modelling window restricts the ability of the methods to reduce the impact of DEM random errors, and to remove DEM outliers in terrain modelling processes.

In this paper, a 2-D Kalman smoothing algorithm for terrain surface modelling is presented, which is a further development of the 2-D Kalman filtering algorithm for terrain modelling, introduced earlier by the authors of this paper (Wang, 1998, Wang et al, 1998a, 1998b, 1999). The 2-D Kalman filtering algorithm had established a stochastic terrain model based on the stochastic characteristics of the grid DEM and terrain geometry, taking into account the effects of DEM random noise and outliers, as well as terrain uncertainty. The 2-D Kalman smoother is a linear combination of the

results of the 2-D Kalman filtering, is able to use all DEM data to generate the optimal estimates of terrain variables of each DEM point, and therefore further improves the accuracy of the derivation of terrain models.

## 2 2-D KALMAN SMOOTHING FOR TERRAIN MODELLING

### 2.1 2-D Kalman filtering for terrain modelling

According to Wang et al (1999), the optimal estimates of elevation  $H(i, j)$ , the first partial derivatives of elevation along the X and Y axes  $H_x(i, j)$  and  $H_y(i, j)$ , of the point  $(i, j)$  of a N x M sized DEM could be recursively derived by the following Kalman equations (see Figure 1(a)).

$$\begin{aligned}
 \mathbf{S}_x^-(i, j) &= \Phi_x(i, j)\mathbf{S}^+(i-1, j) & 1 \\
 \mathbf{P}_x^-(i, j) &= \Phi_x(i, j)\mathbf{P}^+(i-1, j)\Phi_x^T(i, j) + \mathbf{Q}_x(i, j) & 2 \\
 \mathbf{S}_y^-(i, j) &= \Phi_y(i, j)\mathbf{S}^+(i, j-1) & 3 \\
 \mathbf{P}_y^-(i, j) &= \Phi_y(i, j)\mathbf{P}^+(i, j-1)\Phi_y^T(i, j) + \mathbf{Q}_y(i, j) & 4 \\
 \mathbf{S}^-(i, j) &= \mathbf{P}^-(i, j)\left[\left(\mathbf{P}_x^-(i, j)\right)^{-1}\mathbf{S}_x^-(i, j) + \left(\mathbf{P}_y^-(i, j)\right)^{-1}\mathbf{S}_y^-(i, j)\right] & 5 \\
 \mathbf{P}^-(i, j) &= \left[\left(\mathbf{P}_x^-(i, j)\right)^{-1} + \left(\mathbf{P}_y^-(i, j)\right)^{-1}\right]^{-1} & 6 \\
 \mathbf{K}(i, j) &= \mathbf{P}^-(i, j)\mathbf{D}^T(\mathbf{D}\mathbf{P}^-(i, j)\mathbf{D}^T + R(i, j))^{-1} & 7 \\
 \mathbf{S}^+(i, j) &= \mathbf{S}^-(i, j) + \mathbf{K}(i, j)(Z(i, j) - \mathbf{D}\mathbf{S}^-(i, j)) & 8 \\
 \mathbf{P}^+(i, j) &= (\mathbf{I} - \mathbf{K}(i, j)\mathbf{D})\mathbf{P}^-(i, j) & 9
 \end{aligned}$$

where  $\mathbf{S}(i, j)$  is the vector form of the three modelling terrain variables, and called state vector.  $\mathbf{P}(i, j)$  is the variance-covariance matrix associated with  $\mathbf{S}(i, j)$ . The symbol '-' denotes the predicted value of the relevant state vector, or the associated  $\mathbf{P}$  matrix, while symbol '+' represents the updated value of the state vector or the associated  $\mathbf{P}$  matrix.  $\mathbf{K}(i, j)$  is the Kalman gain.  $\mathbf{Q}(i, j)$  and  $R(i, j)$  are the model variance-covariance matrix and the observation variance. 'x' and 'y' indicate the X and Y direction, respectively. The system matrix  $\Phi_x(i, j)$  and  $\Phi_y(i, j)$  are set as

$$\Phi_x(i, j) = \begin{bmatrix} 1 & dx & 0 \\ 0 & 1 & 0 \\ 0 & 0 & 1 \end{bmatrix} \text{ and } \Phi_y(i, j) = \begin{bmatrix} 1 & 0 & dy \\ 0 & 1 & 0 \\ 0 & 0 & 1 \end{bmatrix}, \text{ while } dx \text{ and } dy \text{ are the DEM sampling intervals in the X and Y axes. } \mathbf{D} = \begin{bmatrix} 1 & 0 & 0 \end{bmatrix} \text{ is the design vector.}$$

A procedure for outlier detection and removal had been added into the above Kalman filter. An innovation series  $L(i, j)$  is formed, and used as a test statistic to detect outliers in elevation measurements.

$$L(i, j) = Z(i, j) - \mathbf{D}\mathbf{S}^-(i, j) \quad 10$$

where  $\mathbf{D}\mathbf{S}^-(i, j)$  is the predicted estimate of elevation.

An outlier is detected by the following equation

$$|L(i, j)| > \xi_\alpha \sigma_{L(i, j)} \quad 11$$

where  $\xi_\alpha$  is a critical value with a risk level  $\alpha$ .  $\sigma_{L(i, j)}$  is the standard deviation of  $L(i, j)$ , which can be derived as

$$\sigma_{L(i, j)} = \sqrt{\mathbf{D}\mathbf{P}^-(i, j)\mathbf{D}^T + R(i, j)} \quad 12$$

To remove an outlier, the algorithm amplifies the observation error  $R(i, j)$  into a large value in Eq.7, in order to derive the estimate of elevation mainly based on the predicted estimate of elevation  $DS^-(i, j)$ , ignoring the contribution of the elevation measurement, which is an outlier.

### 2.2 2-D Kalman smoothing algorithm

The shortcoming of applying this 2-D Kalman filter for terrain modelling is that the filter “unevenly” uses the DEM measurements. Some are used only once and others twice. However, modelling the terrain surface using DEMs is mostly an off-line data process. It is of practical interest to incorporate all elevation measurements of a DEM to yield the best estimate of the state vector of each DEM grid point.

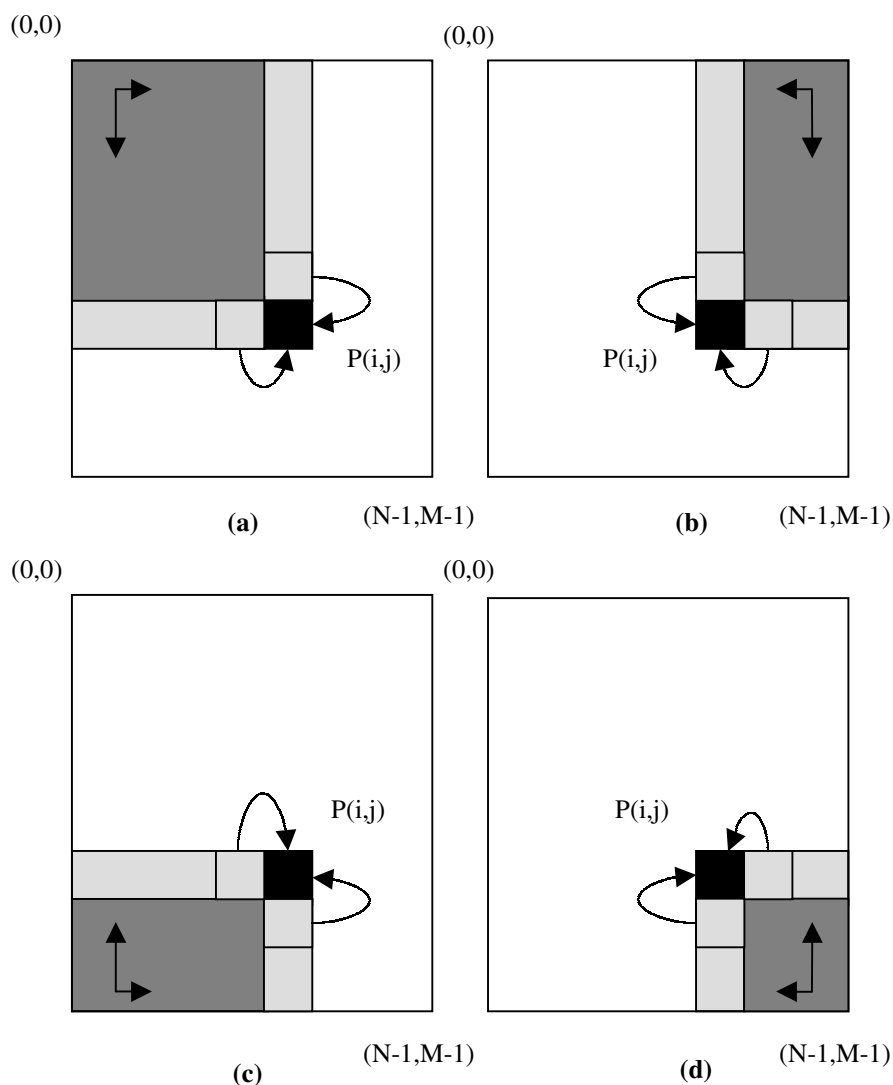


Figure 1. 2-D Kalman smoothing algorithm

To overcome this problem, a 2-D Kalman smoothing algorithm was developed based on the extended 2-D Kalman filter, which includes the outlier detection and removal process. This 2-D Kalman smoothing algorithm uses the 2-D Kalman filter to process a DEM at four different orientations as illustrated in Figure 1. Suppose that the first 2-D Kalman filtering process of the DEM uses orientation 1, based the observations of elevation of the shaded area in Figure 1(a), and derives the updated estimate of the state vector of point  $(i, j)$ , i.e.  $S_1^+(i, j)$ , and the associated variance-covariance matrix  $P_1^+(i, j)$ . Then independently applying the 2-D Kalman filter at the other three orientations shown in Figure 1(b), Figure 1(c) and Figure 1(d),  $S_2^-(i, j)$  together with  $P_2^-(i, j)$ ,  $S_3^+(i, j)$  with  $P_3^+(i, j)$ , and  $S_4^-(i, j)$  with  $P_4^-(i, j)$  will be derived respectively. The Kalman smoother linearly combines the state vector of  $S_1^+(i, j)$ ,  $S_2^-(i, j)$ ,  $S_3^+(i, j)$ , and  $S_4^-(i, j)$  to derive the final estimate  $S_{final}(i, j)$ :

$$\mathbf{S}_{final}(i, j) = \mathbf{P}_{final}(i, j) \left[ \begin{aligned} & \left( \mathbf{P}_1^+(i, j) \right)^{-1} \mathbf{S}_1^+(i, j) + \left( \mathbf{P}_2^-(i, j) \right)^{-1} \mathbf{S}_2^-(i, j) \\ & + \left( \mathbf{P}_3^+(i, j) \right)^{-1} \mathbf{S}_3^+(i, j) + \left( \mathbf{P}_4^-(i, j) \right)^{-1} \mathbf{S}_4^-(i, j) \end{aligned} \right] \quad 13$$

$$\mathbf{P}_{final}(i, j) = \left[ \left( \mathbf{P}_1^+(i, j) \right)^{-1} + \left( \mathbf{P}_2^-(i, j) \right)^{-1} + \left( \mathbf{P}_3^+(i, j) \right)^{-1} + \left( \mathbf{P}_4^-(i, j) \right)^{-1} \right]^{-1} \quad 14$$

Here  $\mathbf{S}_1^+(i, j)$  and  $\mathbf{S}_3^+(i, j)$  are the a posteriori estimates derived from the filtering using orientations 1 and 3, and their associated  $\mathbf{P}_1^+(i, j)$  and  $\mathbf{P}_3^+(i, j)$  are also the a posteriori variance covariance matrixes. However,  $\mathbf{S}_2^-(i, j)$  and  $\mathbf{S}_4^-(i, j)$  are the a priori estimates derived from the filtering of orientation 2 and 4, which do not use the elevation measurement of  $Z(i, j)$ , because it has been already used in the derivation of  $\mathbf{S}_1^+(i, j)$  and  $\mathbf{S}_3^+(i, j)$ .

In this way, the elevation measurement of  $Z(i, j)$  has been used twice in deriving the final estimate  $\mathbf{S}_{final}(i, j)$  and  $\mathbf{P}_{final}(i, j)$ . For the rest of the  $i$  th row and  $j$  th column of the DEM, the elevation measurements have also been used twice, since this row and column overlap the area of the four filtering processes and have been used once in each of the relevant filtering steps. Therefore, the whole DEM data are used twice to generate the estimates of terrain variables of every DEM point by 2-D Kalman smoother. In this case, the variance of the observations should be modified to half of the actual value for each filtering process, when the smoothing procedure is applied.

The results of  $\mathbf{S}_{final}(i, j)$  and  $\mathbf{P}_{final}(i, j)$  are independent of the choice of two predict estimates and two updated estimates from the four filtering processes. Eq. 13 and Eq. 14 are only one example of how to choose the estimates and the relevant variance-covariance matrix. The smoother produces the same result using any two predict  $\mathbf{S}^-(i, j)$  and  $\mathbf{P}^-(i, j)$  of four processing orientations, and two updated  $\mathbf{S}^+(i, j)$  and  $\mathbf{P}^+(i, j)$  of the other two orientations.

### 3 EXPERIMENTS

Due to the difficulty of obtaining the ground truth of elevations, and the relevant first partial derivatives of a real terrain surface, an artificial terrain surface was simulated to test the efficiency of the 2-D Kalman smoothing, in terms of reducing the effect of DEM random noise and removing the impact of DEM outliers on the derivation of terrain variables. The surface has 150 by 150 DEM points sampled with 1m interval in both X and Y directions. The elevation changes between -18.32 m and 18.56 m, with 0.03 m as the average height. It has two flat first partial derivative surfaces with 0.06 mean for the one along the X axis and zero mean for the Y axis. Random noise with 0.5 metre standard deviation and five outliers were added to the simulated DEM, resulting in a noisy DEM (see Figure 2) to be processed by the 2-D Kalman smoothing algorithm.

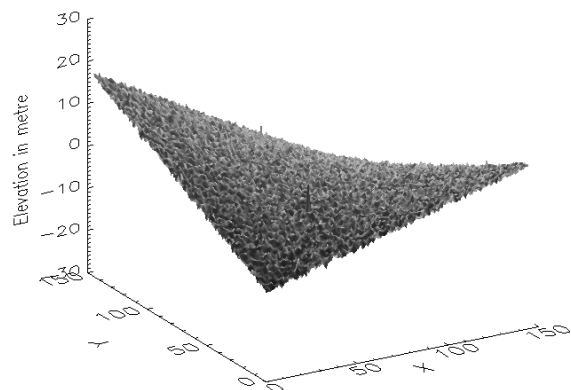
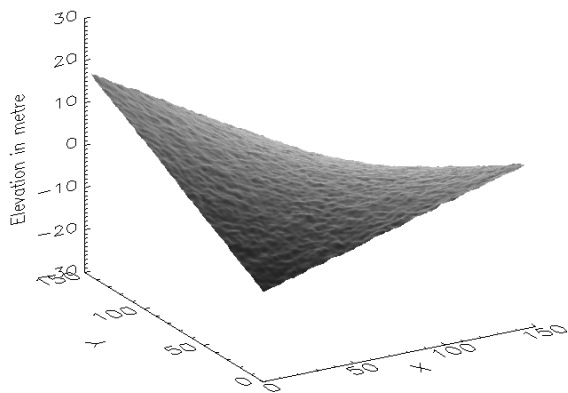


Figure 2. The simulated noisy DEM

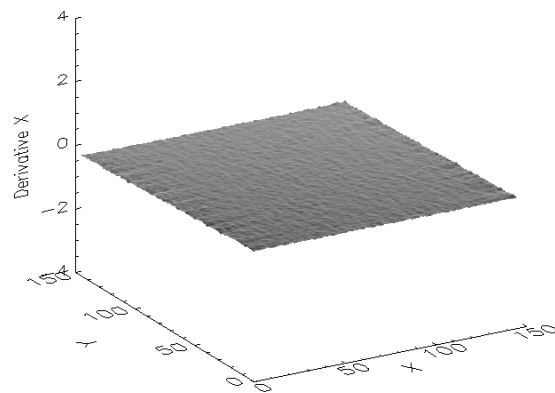
Applying the 2-D Kalman smoothing algorithm over the noisy test DEM data, the 2-D Kalman smoother produced simultaneously the estimates of elevation, and the derivatives of the X and Y surfaces illustrated in Figure 3. The two later estimates were used to compute the estimates of slope and aspect using the following equations.

$$slope(i, j) = 180 \times atan \left( \sqrt{(H_x(i, j))^2 + (H_y(i, j))^2} \right) / \pi \quad 15$$

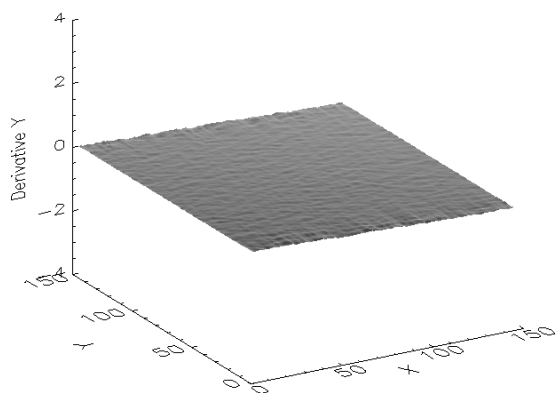
$$aspect(i, j) = \begin{cases} 180 \times atan \left( \frac{H_y(i, j)}{H_x(i, j)} \right) / \pi & \text{if } H_x(i, j) \neq 0 \\ -100 & \text{if } H_x(i, j) = 0 \end{cases} \quad 16$$



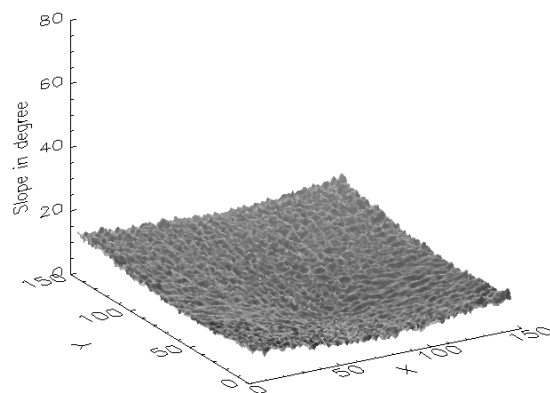
(a) Elevation



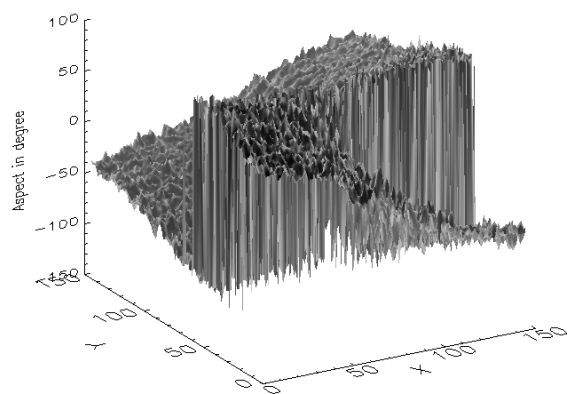
(b) Derivative X



(c) Derivative Y



(d) Slope



(e) Aspect

Figure 3. Results of the application of 2-D Kalman smoothing algorithm

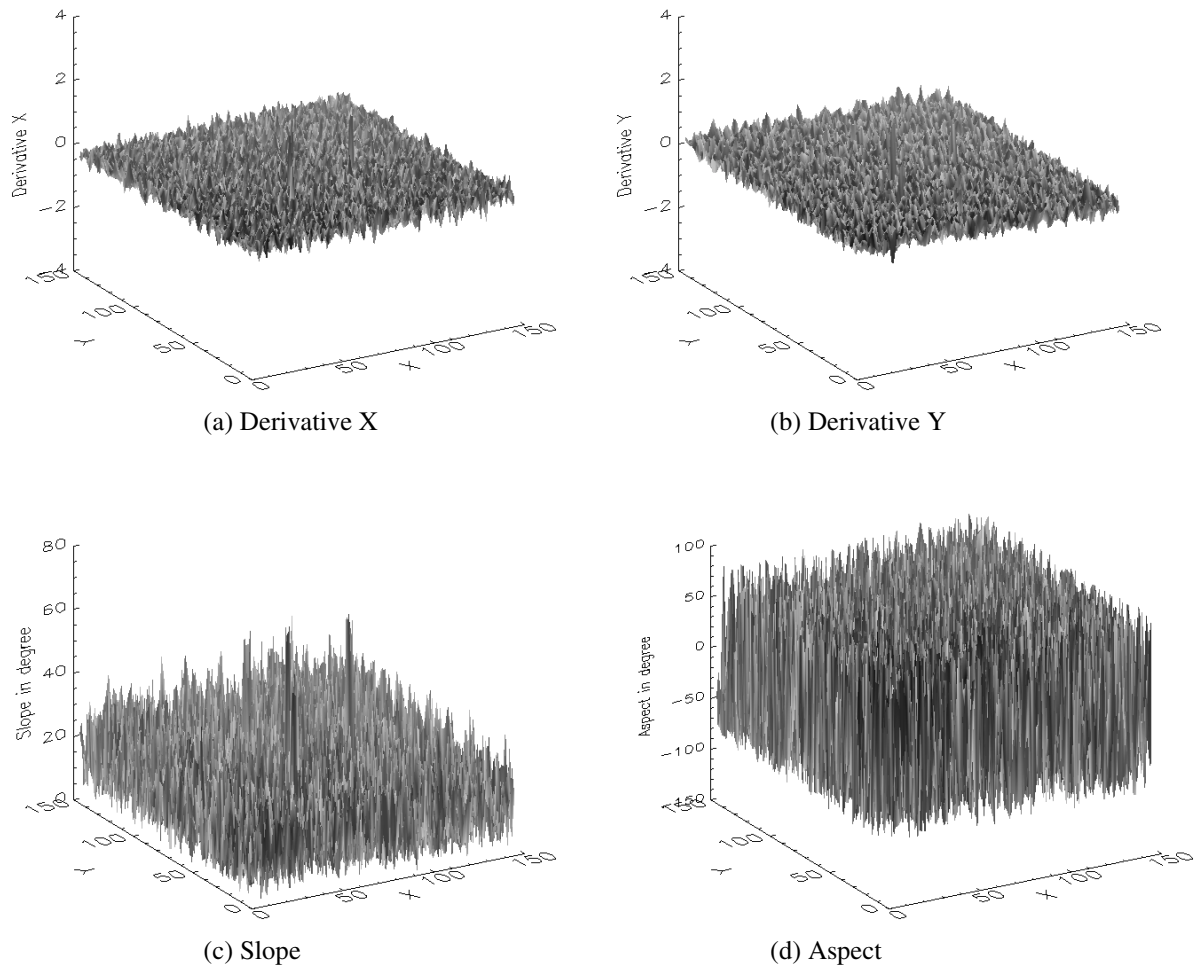


Figure 4. Results of the application of the Evans' model

The smoothing result indicates the extent of the smoothing and accuracy of the terrain surfaces, derivatives of X and Y, slope and aspect, compared with the relevant ground truth. The significant improvement after the Kalman smoothing appears at the four boundaries, and this is due to the linear combination of the four filtering results.

The results of the 2-D Kalman smoothing algorithm on the noisy DEM were compared with those of the Evans' model, which is currently judged by Florinsky (1998) to be the most accurate terrain model. The Evans' model does not provide the estimates of elevation, but generated the estimates of the derivative X and Y, slope and aspect from the noisy test data as shown in Figure 4. The results of the application of the Evans' model displayed strong influences of DEM outliers as well as DEM random noise. The derived derivatives of X and Y are considerably noisy compared with the ground truth, while the slope and aspect surface are even worse, producing both incorrect slope and aspect patterns.

Using the ground truth of the first partial derivatives of elevation, and slope and aspect, by subtracting the respective results of the 2-D Kalman smoothing and the Evans' model, errors in the derived derivative X and Y, slope and aspect were obtained, as summarized in Table 1. Similarly, errors in the estimates of elevation following the 2-D Kalman smoothing and the test DEM data were obtained, using the ground truth elevations, by subtracting the results of the 2-D Kalman smoothing and the test data, which were also listed in Table 1. Since the Evans' model is not able to produce estimates of elevations, the efficiency of the elevation computation of the 2-D Kalman smoothing was compared with the elevation ground truth.

The statistical analysis of the results of the 2-D Kalman smoothing indicates that the 2-D Kalman smoothing algorithm is significant in terms of reducing the DEM random noise and detection and removal of DEM outliers. The standard deviation of the errors remained in the elevations following 2-D Kalman smoothing had been reduced by 78%, compared with those existing in the noisy test data.

The 2-D Kalman smoothing algorithm produced better terrain variables than the Evans' model. The accuracy of the derivative in X and Y, slope and aspect of the 2-D Kalman smoothed data has also been greatly improved compared with those derived by the Evans' model. The improvement of the data following 2-D Kalman smoothing over that derived using the Evans' model, is as much as 95% for both derivative X and Y, 92% for slope and 62% for estimates of aspect.

	Minimum value	Maximum value	Mean value	Standard deviation	Improvement
<b>Elevation</b>					
Test DEM data*	-7.51m	11.00m	0.00m	0.51m	---
Kalman smoothing	-0.44m	0.45m	0.00m	0.11m	<b>78%</b>
<b>Derivative X</b>					
Evans' model	-1.70	2.00	0.00	0.21	---
Kalman smoothing	-0.09	0.06	-0.01	0.01	<b>95%</b>
<b>Derivative Y</b>					
Evans' model	-2.08	1.97	0.00	0.21	---
Kalman smoothing	-0.06	0.06	0.00	0.01	<b>95%</b>
<b>Slope</b>					
Evans' model	-67.08degree	15.33degree	-7.62degree	8.09degree	---
Kalman smoothing	-1.83degree	4.26degree	0.90degree	0.63degree	<b>92%</b>
<b>Aspect</b>					
Evans' model	-177.27degree	177.69degree	-0.42degree	68.53degree	---
Kalman smoothing	-178.70degree	178.62degree	0.40degree	25.74degree	<b>62%</b>

\*Here errors refer to the random errors and outliers added to the test DEM data.

Table 1. Errors in the results of the 2-D Kalman smoothing algorithm and the Evans' model

#### 4 CONCLUSIONS

A 2-D Kalman smoothing algorithm for terrain surface modelling using grid DEMs is introduced. It is based on the 2-D Kalman filtering algorithm previously developed by the authors of the paper. The 2-D Kalman smoother is a linear combination of four filtering results, and is able to use all DEM data to estimate terrain variables of each DEM point. Therefore, it further improves the accuracy of derived terrain variables compared with the 2-D Kalman filter for the noisy DEM.

The experimental results over a simulated surface indicates that the 2-D Kalman smoothing algorithm produces much more accurate terrain variables than the Evans' model. The improvement of the 2-D Kalman smoothing, compared with the Evans' model, is 95% for the computation of the first partial derivatives of elevation, 92% for the derivation of the relevant slope surface, and 62% for the aspect surface calculation.

#### REFERENCES

- Chang, K., Tsai, B., 1991. The effect of DEM resolution on slope and aspect mapping. *Cartography and Geographic Information Systems* 18(1), pp. 69-77.
- Florinsky, I.V., 1998. Accuracy of local topographic variables derived from Digital Elevation Models. *International Journal of Geographical Information Science* 12(1), pp. 47-61.
- Hawkins, D.M., 1980. Identification of outliers. Chapman and Hall, New York, pp1-9.
- Hunter, G.J., Goodchild, M.F., 1997. Modeling the uncertainty of slope and aspect estimates derived from spatial databases. *Geographical Analysis*, 29(1), pp. 35-49.
- Kraus, K., 1994. Visualization of the quality of surfaces and their derivatives. *Photogrammetric Engineering and Remote Sensing*, 60(4), pp.457-462.

- Lee, J., Snyder, P.K., Fisher, P.F., 1992. Modeling the effect of data errors on feature extraction from Digital Elevation Models. *Photogrammetric Engineering and Remote Sensing*, 58(10), pp. 1461-1467.
- Li, Z., 1994. A comparative study of the accuracy of Digital Terrain Models (DTMs) based on various data models. *ISPRS Journal of Photogrammetry and Remote Sensing*, 49(1), pp. 2-11.
- Moore, I.D., Grayson, R.B., Ladson, A.R., 1991. Digital Elevation Model: a review of hydrological, geomorphological and biological applications. *Hydrological Processes* 5, pp. 3-30.
- Rieger, W., 1996. Accuracy of slope information derived from DEM-data. In: *International Archives of Photogrammetry and Remote Sensing*, Vienna, Vol. 31, Part 4, pp. 690-695.
- Skidmore, A.K., 1989. A comparison of techniques for calculating gradient and aspect from a gridded Digital Elevation Model. *International Journal of Geographical Information Systems*, 3(4), pp. 323-334.
- Srinivasan, R., Engel, B.A., 1991. Effect of slope prediction methods on slope and erosion estimates. *Applied Engineering in Agriculture*, 7(6), pp. 779-783.
- Tempfli, K., 1980. Spectral analysis of terrain relief for the accuracy estimation of Digital Terrain Models, *ITC Journal*, 1980-3, pp. 478-510
- Torlegård, K., Östman, A., Lindgren, R., 1986. A comparative test of photogrammetrically sampled Digital Elevation Models. *Photogrammetria*, 41, pp. 1-16.
- Wang, P., 1998. Applying two dimensional Kalman filtering on Digital Elevation Models. In: *International Archives of Photogrammetry and Remote Sensing*, Vol. 32, Part 4, pp. 649-656.
- Wang, P., Trinder, J.C., Han, S. 1998a. A two dimensional Kalman filtering approach to derivation of terrain surface variables. In: the 9th Australian Remote Sensing and Photogrammetry Conference, Sydney, Australia. Proceedings CD-ROM, Volume 1, paper no. 56, 14 pages.
- Wang, P., Trinder, J.C., Han, S., 1998b. DEM outlier detection, identification and adaptation using digital signal processing technology. In: *Proceedings of 39th Australian Surveyors Congress*, Launceston, Australia, pp. 269-276.
- Wang, P., Trinder, J.C., Han, S., 1999. A two-dimensional Kalman filtering algorithm for terrain surface modelling using Digital Elevation Models. Submitted to the *ISPRS Journal of Photogrammetry and remote Sensing*.